Journal of Biomechanics 82 (2019) 134–141

Contents lists available at ScienceDirect

Journal of Biomechanics

journal homepage: www.elsevier.com/locate/jbiomech
www.JBiomech.com

Experimental evaluation of pressure drop for flows of air and heliox through upper and central conducting airway replicas of 4- to 8-year-old children

Tyler Paxman [a], Michelle Noga [b], Warren H. Finlay [a], Andrew R. Martin [a,*]

[a] Department of Mechanical Engineering, University of Alberta, Canada
[b] Department of Radiology & Diagnostic Imaging, University of Alberta, Canada

ARTICLE INFO

Article history:
Accepted 20 October 2018

Keywords:
Airway resistance
Pressure drop
Blasius
Breathing

ABSTRACT

Airway resistance describes the ratio between pressure drop and flow rate through the conducting respiratory airways. Analytical models of airway resistance for tracheobronchial airways have previously been developed and assessed without upper airways positioned upstream of the trachea. This work investigated pressure drop as a function of flow rate and gas properties for upper and central airway replicas of 10 child subjects, ages 4–8. Replica geometries were built based on computed tomography scan data and included airways from the nose through 3–5 distal branching airway generations. Pressure drop through the replicas was measured for constant inspiratory flows of air and heliox. For both the nose-throat and branching airways, the relationship between non-dimensional coefficient of friction, C_F, with Reynolds number, Re, was found to resemble the turbulent Blasius equation for pipe flow, where $C_F \propto Re^{-0.25}$. Additionally, pressure drop ratios between heliox and air were consistent with analytical predictions for turbulent flow. The presence of turbulence in the branching airways likely resulted from convection of turbulence produced upstream in the nose and throat. An airway resistance model based on the Blasius pipe friction correlation for turbulent flow was proposed for prediction of pressure drop through the branching bronchial airways downstream from the upper airway.

1. Introduction

Airway resistance, the ratio between pressure drop and flow rate through the conducting airways, is an important quantity used in describing respiratory mechanics. Assessment of airway resistance is used in diagnosis of respiratory diseases, and in evaluation of their progression and treatment. Increased airway resistance contributes to increased work of breathing in obstructive lung disease. Variation in airway resistance between airways or lung regions can influence ventilation distribution, which in turn affects regional gas transport and exchange (Tgavalekos et al., 2007). Analytical models of airway resistance have been used to predict the pressure distribution through the conducting airways as a function of flow rate and gas properties (Gemci et al., 2008; Katz et al., 2012; Katz et al., 2011b; Litwin et al., 2017), to assess the contribution of heterogeneous airway resistance to ventilation distribution (Pozin et al., 2017; Swan et al., 2012; Wongviriyawong et al., 2012), and to optimize algorithms predicting alveolar pressure during mechanical ventilation (Damanhuri et al., 2014).

Development and validation of analytical airway resistance models has focused primarily on adults. Pedley et al. (1970) proposed a correction to the Hagen-Poiseuille equation to estimate pressure drop due to viscous energy dissipation through bifurcating airways as a function of airway dimensions, gas properties, and flow rate. Van Ertbruggen et al. (2005) simulated pressure drop through an adult tracheobronchial airway tree, and proposed modified coefficients for the Pedley et al. (1970) equation. Recent work was done by Borojeni et al. (2015) to compare predictions of these models to pressure drop measured experimentally through adult and child conducting airway replicas. Borojeni et al. found the predictions of the van Ertbruggen model were in reasonable agreement with measurements for adults, while for children, the original Pedley model most closely matched experimental data, though with a tendency to under predict measured pressure drop.

A limitation of the experiments done by Borojeni et al. (2015), and in the work of Pedley et al. (1970) and van Ertbruggen et al. (2005), is the omission of an upper airway upstream from the

* Corresponding author. Address: 10-324 Donadeo Innovation Centre for Engineering, 9211-116 Street NW, Edmonton, Alberta T6G 1H9, Canada.
E-mail addresses: tpaxman@ualberta.ca (T. Paxman), armartin@ualberta.ca (A.R. Martin).

https://doi.org/10.1016/j.jbiomech.2018.10.028
0021-9290/

trachea. In computational studies, turbulence generated in the upper airway has been observed to influence flow patterns in the trachea and bronchi (Calmet et al., 2016; Koullapis et al., 2017; Lin et al., 2007; Xi et al., 2008). The suitability of existing airway resistance models for predicting pressure drop through conducting airways downstream from realistic upper airways is therefore not known.

In the work reported here, pressure drop was measured for varying gas flow rates through realistic conducting airway replicas that included the nose-throat airway, trachea, and bronchial airways terminating, on average, between generations 3 and 5. Replicas were based on computed tomography (CT) scans of 10 child subjects, between 4- and 8-years old. Experiments were conducted with both air and a helium/oxygen mixture (heliox). A dimensionless friction coefficient (Slutsky et al., 1980) was analysed as a function of tracheal Reynolds number to investigate the functional form of the pressure drop behaviour through the tracheobronchial airways. An airway resistance model based on the Blasius pipe friction correlation (White, 2016) is proposed for prediction of pressure drop through the bifurcating bronchial airways downstream from the upper airway.

2. Methods

2.1. Child airway replicas

The airway replicas were created from CT scan data of the same 10 child subjects studied by Borojeni et al. (2015). The extraction of data from the CT scans to create 3D model (STL) files was done with the approval of the Health Research Ethics Board (HREB) of the University of Alberta, as described in previous work by Borojeni et al. (2014). In the present work, new models were built from the same CT scan source data for 10 child subjects, with the upper airway of the nose and throat included. Demographic and geometric data are listed in Table 1.

The replicas were produced with a 3D printer (Objet Eden 350 V, Stratasys Ltd., MN, USA), using a rigid opaque photopolymer material (VeroGray, Stratasys Ltd., MN, USA). The printing of each replica was done in three parts, where the top and middle pieces comprised the airways from the nasal inlet to the end of the trachea, and the bottom piece consisted of all branching airways (up to an average of 3–5 generations, depending on the subject replica). These three pieces were fastened to create a single airway geometry. This modular printing facilitated removal of support material after printing and allowed for measurements with the bottom branching airways either attached or detached. A summary of the range and average dimensions in each branching generation (from 0 to 5) is provided in Table 2. In addition, the dimensions of the upper airways of each subject are characterized by cross-sectional areas at selected points as shown in Table 3, where areas for the nostrils are defined as the sum of both nasal inlets, the nasal valve is a local minimum of cross-sectional area between the nasal vestibule and turbinates (Bates et al., 2015; Xi et al., 2011), and measurement of the nasopharynx area was selected immediately posterior to the connection of the nasal passages.

After printing, support material was removed manually, assisted by using a sonic bath. To verify that the support material was removed from the internal airways, the printed models were scanned using CT (SOMATOM Definition Flash CT Scanner, Siemens, Munich, Germany), converted to 3D models, and then compared with original 3D models using CAD software (3-matic, Materialise, Leuven, Belgium). It was concluded that negligible amounts of support material remained in the main air passages of the replicas. Support material did remain in the sinus cavities; however, this was assumed to have no influence on airflow through the replicas. We have previously shown that the present fabrication method provides built airways that closely match the CT source airways (Storey-Bishoff et al., 2008). The printed replicas are shown in Fig. 1.

2.2. Apparatus

A rotary vane vacuum pump (Gast Model 0523, Gast Manufacturing, MI, USA) was used to draw unidirectional airflow through the replica, with a needle valve and mass flow meter (TSI Model 4043; TSI; MN, USA) used to set the flow rate. A cylindrical plastic chamber housed the airway replica. For each test, the airway replica was placed in the chamber, suspended and sealed midway

Table 1
Physical properties for each child subject.

Subject number	Tracheal length (mm)	Tracheal diameter (mm)	Age	Sex	Height (m)	Weight (kg)
2	79.9	7.05	5	M	1.17	22.9
3	79.5	7.99	5	M	1.12	20.0
5	71.5	7.99	6	F	1.12	18.0
6	78.0	8.50	6	F	1.18	21.5
9	76.4	7.56	5	M	1.13	20.0
10	70.7	7.15	4	F	0.99	16.0
11	81.9	10.5	8	M	1.25	24.5
12	90.6	7.41	6	F	1.24	24.0
13	87.5	9.78	7	F	1.21	20.0
14	75.2	7.16	4	F	1.00	16.0

Table 2
Summary of diameters, lengths, and number of airways at each generation for the branching airways of all subject replicas.

Generation number	Number of airways	Diameters (mm)				Lengths (mm)			
	Avg. per subject	Min.	Max.	Avg.	Std.	Min.	Max.	Avg.	Std.
0	1	7.05	10.49	8.11	1.17	70.7	90.6	79.12	6.36
1	2	3.45	11.54	6.26	2.08	6.9	41.3	25.32	12.38
2	4	3.02	8.27	5.14	1.26	2.8	21.6	8.98	4.21
3	8	1.40	11.37	4.51	1.92	1.3	26.4	9.20	5.81
4*	10	0.69	8.90	3.81	1.67	1.1	34.6	10.26	6.26
5*	9	0.73	10.75	3.32	1.83	1.3	21.8	10.26	5.44

* *Note*: some paths in the branching airways of a given subject do not contain more than 3 generations.

Table 3
Cross-sectional areas of upper airway geometries of each subject at the trachea, nasopharynx, nasal valve and nostrils, measured from 3D model STL geometry files.

Subject number	Cross-sectional area (mm^2)			
	Trachea	Nasopharynx	Nasal valve	Nostrils
2	42	180	100	55
3	49	170	72	115
5	47	75	98	85
6	60	207	91	66
9	46	220	82	80
10	30	141	99	58
11	91	310	119	100
12	43	186	67	86
13	77	211	179	84
14	39	142	88	56
Minimum	30	75	67	55
Maximum	91	310	179	115
Mean	52	184	99	78
Standard deviation	17	58	30	19

Fig. 1. 3D-printed airway replicas of all child subjects (top row, left to right: subjects 2, 3, 5, 6, and 9; bottom row, left to right: subjects 10, 11, 12, 13, and 14).

around the trachea, such that branching airways were contained within the sealed chamber, with the nasal inlet outside the chamber.

Both room air and heliox (80/20 helium/oxygen mixture, by volume) were used in the experimental procedure. Each replica was fitted with a mask (Infant Pocket Mask, nSpire Health Inc., CO, USA) sealed to the face with silicone, as visible in Fig. 1. For heliox, a Douglas Bag (1196 Series, VacuMed, CA, USA) was filled from a compressed cylinder and connected to the mask via large-bore tubing. For air, the mask was left open to the room air. Preliminary tests drawing air from the room versus the Douglas bag produced indistinguishable results. Pressure drop across the replicas was measured using a digital manometer (HHP-103, Omega Engineering, CT, USA). A schematic of the experimental apparatus is show in Fig. 2.

2.3. Experimental procedure

After installing a replica into the chamber, pressure drop (ΔP) was recorded for standard flow rates of 5, 10, 15, and 30 L/min for air, and 7, 14, 23, and 46 L/min for heliox. This was repeated for each replica, in two configurations: with the branching airway segment (bottom) either attached or detached (yielding ΔP_{attach} and ΔP_{detach}, respectively). These two measurements were used to obtain values for the pressure drop over the branching and nose-throat airways ($\Delta P_{Branches}$ and ΔP_{NT}, respectively), using the following formulae:

$$\Delta P_{NT} = \Delta P_{detach} - \Delta P_{SE} - \Delta P_{open} \quad (1)$$

$$\Delta P_{Branches} = \Delta P_{attach} - \Delta P_{detach} + \Delta P_{SE} \quad (2)$$

ΔP_{SE} is the sudden expansion pressure loss, which accounts for the losses occurring when the gas exits the trachea and expands into the plenum when in the detached-configuration:

$$\Delta P_{SE} = \frac{1}{2}\rho K_{SE} v_{exit}^2 \quad (3)$$

where v_{exit} is the velocity at the exit, and K_{SE} is the sudden expansion coefficient—set to 1 in all cases. ΔP_{open} is the pressure drop recorded across the chamber in the absence of any replica, and accounts for the losses in the short outlet connection between the chamber and pressure tap. Measurements were made in triplicate for each unique experimental arrangement (i.e. for a given flow rate, gas type, and replica configuration).

2.4. Pressure drop dependence on Reynolds number

The Reynolds number was defined using tracheal diameter as follows:

$$Re = \frac{\rho v d_{trachea}}{\mu} = \frac{4\rho Q}{\pi \mu d_{trachea}} \quad (4)$$

where μ and ρ are the fluid viscosity and density, respectively, $d_{trachea}$ is the tracheal diameter, and v and Q are fluid velocity and flow rate, respectively. The maximum, minimum, and mean Reynolds numbers for the ten subjects are listed in Table 4 for each fluid and flow rate.

The non-dimensional coefficient of friction (C_F) defined by Slutsky et al. (1980) is:

$$C_F = \frac{\Delta P}{1/2\rho(Q^2/A^2)} \quad (5)$$

where ΔP is the pressure drop across the branching airways and A is the tracheal cross-sectional area. This friction coefficient may be related to Reynolds number using an alternate form of the Weisbach equation (White, 2016):

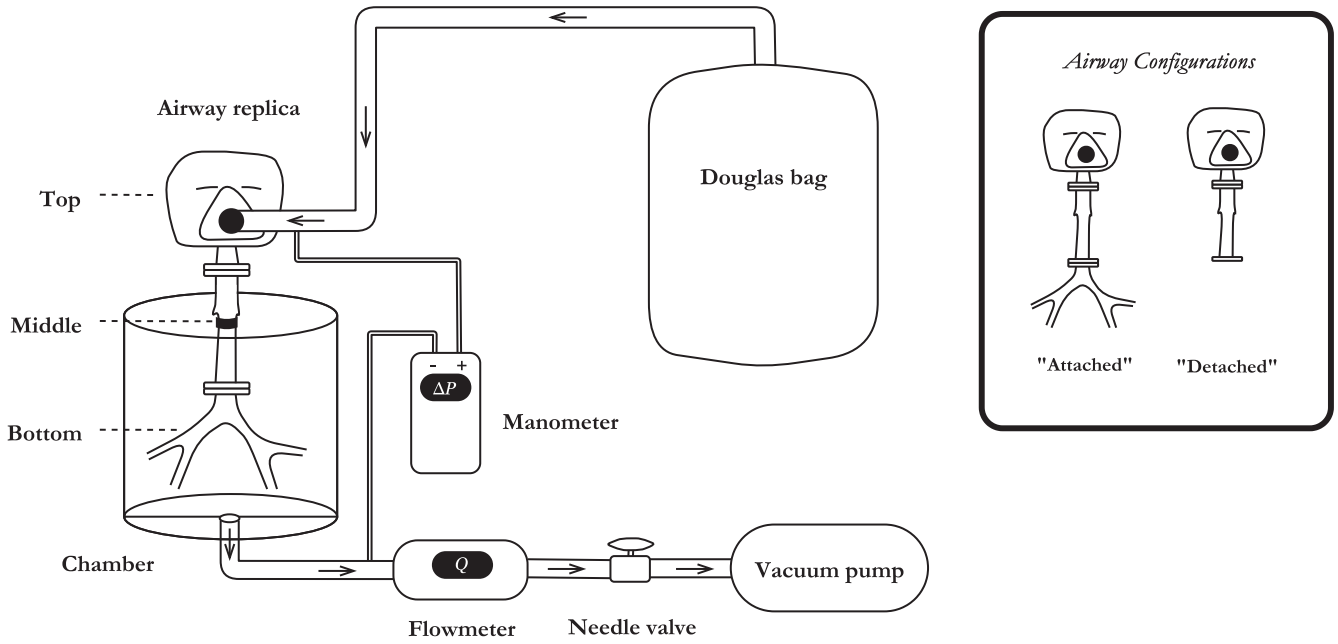

Fig. 2. Experimental apparatus schematic illustrating the measurement of pressure drop across child airway replicas.

Table 4
Range of tracheal Reynolds numbers for each fluid and nominal flow rate.

	Nominal Q (L/min)	Re_{max}	Re_{min}	Re_{mean}
Air	5	998	671	882
	10	1995	1343	1764
	15	2992	2012	2646
	30	5988	4021	5262
Heliox	7	386	259	341
	14	810	544	716
	23	1276	859	1129
	46	2547	1711	2251

$$C_F = \beta Re^{-\alpha} \tag{6}$$

where α depends on the flow regime and β is some constant related to the airway geometry. From the definition of the Darcy friction factor, it follows that $\alpha = 1$ signifies laminar Poiseuille flow, while $\alpha = 0.25$ denotes turbulent flow, based on the Blasius turbulent equation (Blasius, 1911). By taking the log of Eq. (6), α can be readily extracted from the slope of the line of best fit in the resultant expression:

$$\log(C_F) = \log(\beta) - \alpha \log(Re) \tag{7}$$

2.5. General analytical calculation of pressure drop

An iterative procedure for the calculation of pressure drop in a bifurcating network was adapted from Borojeni et al. (2015). For the calculation, a resistance ratio incorporating pressure drop, fluid density, and the square of flow rate through an individual airway was used:

$$R = \frac{\Delta P}{\rho Q^2} \tag{8}$$

In the present experiments, gas flows from the nasal inlet to the branching airways where it empties into a plenum; as such, the pressure drop through every path in the model must be the same. With this constraint, a system of equations can be derived where each branch is assigned an equivalent resistance, which can be determined as a function of its own resistance and the resistances of all its daughter branches:

$$R_{eq,p} = R_p + \left(R_{eq,a}^{-1/2} + R_{eq,b}^{-1/2}\right)^{-2} \tag{9}$$

where p denotes any parent airway branch, and a and b refer to its daughter branches.

This creates a recursive series of equivalent resistance calculations, where the ultimate branch values (i.e. final generation) are known resistances, defined as $R_{eq,p} = R_p$. The resulting system of non-linear equations is solvable in an iterative procedure, where total pressure drop values across each path ultimately converge to a single value. Flow rates in each branch are initialized assuming equal flow division at each bifurcation. Equivalent resistances are then calculated, beginning with the most distal airways and moving to the trachea, using Eq. (9). Each branch flow rate is then updated as follows, beginning with the trachea and moving distally through the branching airways:

$$Q_a^{i+1} = \left(\frac{R_{eq,b}^{1/2}}{R_{eq,a}^{1/2} + R_{eq,b}^{1/2}}\right)^{i} Q_{inlet}^{i+1} \tag{10}$$

$$Q_b^{i+1} = Q_{inlet}^{i+1} - Q_a^{i+1} \tag{11}$$

where Q_{inlet} is the flow rate of the parent of branches a and b.

Table 5
β-coefficent, α-exponent and R^2 values for each C_F vs. *Re* plot.

Subject number	Branching airways			NT airways		
	β (coefficient)	α (exponent)	R^2	β (coefficient)	α (exponent)	R^2
2	14.68	0.261	0.896	34.64	0.207	0.696
3	12.05	0.183	0.886	64.21	0.261	0.776
5	17.38	0.256	0.829	69.01	0.254	0.773
6	18.93	0.259	0.981	57.29	0.206	0.926
9	20.91	0.225	0.798	67.44	0.116	0.434
10	18.30	0.206	0.903	36.02	0.258	0.870
11	20.45	0.247	0.891	101.94	0.147	0.520
12	28.76	0.251	0.970	100.35	0.222	0.952
13	22.03	0.277	0.844	40.63	0.207	0.583
14	14.02	0.212	0.896	62.00	0.297	0.794

The convergence criterion was defined as the difference of the maximum and minimum pressure drop values across each path, divided by the tracheal pressure drop. A value of less than 10^{-8} was accepted as fully converged, as changes to the difference in pressure drop between paths were found to be negligible below this value.

Comparisons of the predictions of this analytical model with the experimental values were done using the concordance correlation coefficient, ρ_c, developed by Lawrence and Lin (1989). This coefficient ranges from 0 to 1, with a higher value indicating better agreement between experimental measurements and analytical predictions.

2.6. Analytical turbulent flow model determination

Based on analysis presented below of C_F and *Re* in Eqs. (6) and (7), the following equation was defined:

$$f = C_F \frac{d}{L} = CRe_d^{-0.25} \tag{12}$$

where f is the Darcy friction factor, L and d are the length and diameter of an airway segment, and C is a constant. Standard conditions were assumed for gas properties (20 °C, 1 atm). Density and viscosity values used, respectively, were 1.206 kg/m^3 and 1.820×10^{-5} Pa·s for air, and 0.399 kg/m^3 and 2.147×10^{-5} Pa·s for heliox (Katz et al., 2011a).

A modified-Blasius model for pressure drop can be constructed by combining the Weisbach equation (White, 2016) with Eq. (12), as follows:

$$\Delta P = f \frac{L}{d} \frac{\rho v^2}{2} = \frac{C}{Re^{0.25}} \frac{L}{d} \frac{\rho v^2}{2} \tag{13}$$

To determine a value for C, pressure drop was calculated analytically using the modified-Blasius equation in Eq. (13) to define the resistance in Eq. (8), and beginning with an arbitrary initial guess for C. For a given subject, the resultant pressure drop values were then compared with their corresponding experimental pressure drop measurements using the concordance correlation coefficient (ρ_c) to assess their agreement. Iterative adjustments were made to C to optimize ρ_c to a value of 1, indicating equivalence between analytical and experimental data. This process was applied to each subject separately, to obtain an optimal, subject-specific coefficient value for the modified-Blasius model, defined as C_{ideal}.

3. Results

3.1. Experimental pressure drop compared with Reynolds number

Calculations of C_F versus *Re* using nose-throat and branching pressure drop values were used to fit Eq. (7) where the coefficient, β, exponent, α, and R^2 value are shown in Table 5. Exemplary log–log plots of C_F vs. *Re* in Subject 10, for both branching and nose-throat airways, are shown with lines of best fit in Fig. 3.

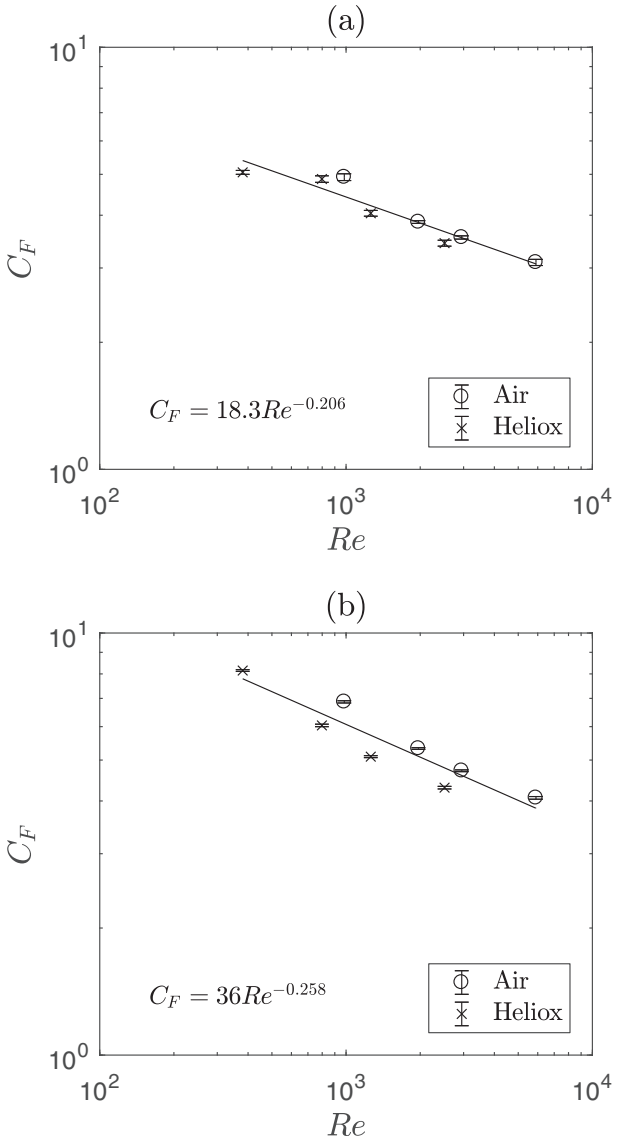

Fig. 3. Log-log plot of friction coefficient, C_F, vs. Reynolds number, *Re*, for subject 10 in (a) branching and (b) nose-throat airways. (Solid lines represent the best fit function indicated in the lower left corner of each plot. Error bars represent standard error. Where error bars are not visible the standard error is less than the size of the data symbol.)

3.2. Analytical calculation of pressure drop and airway resistance

Subject-specific coefficients, C_{ideal}, for the modified-Blasius model ranged from 1.97 to 4.98 among subjects, with an average value of 2.98 and standard deviation of 0.99. Analytical calculations for pressure drop were done for each subject using C_{ideal} in the modified-Blasius formulation, Eq. (13). Analytical vs. experimental pressure drop in the branching airways for all subjects is shown in Fig. 4a. Fig. 4b shows a similar comparison, instead using the average of all subject-specific C_{ideal} values, such that C_{avg} = 2.98 for all subjects.

4. Discussion

4.1. Experimental pressure drop compared with Reynolds number

The aim of this work was to experimentally assess pressure drop behavior in the upper and central airways of children. In particular, pressure drop was assessed in the central branching airways with the anatomically accurate boundary condition of a nose-throat airway upstream from the trachea. The relationship between C_F and Re was evaluated in both the nose-throat and branching airways.

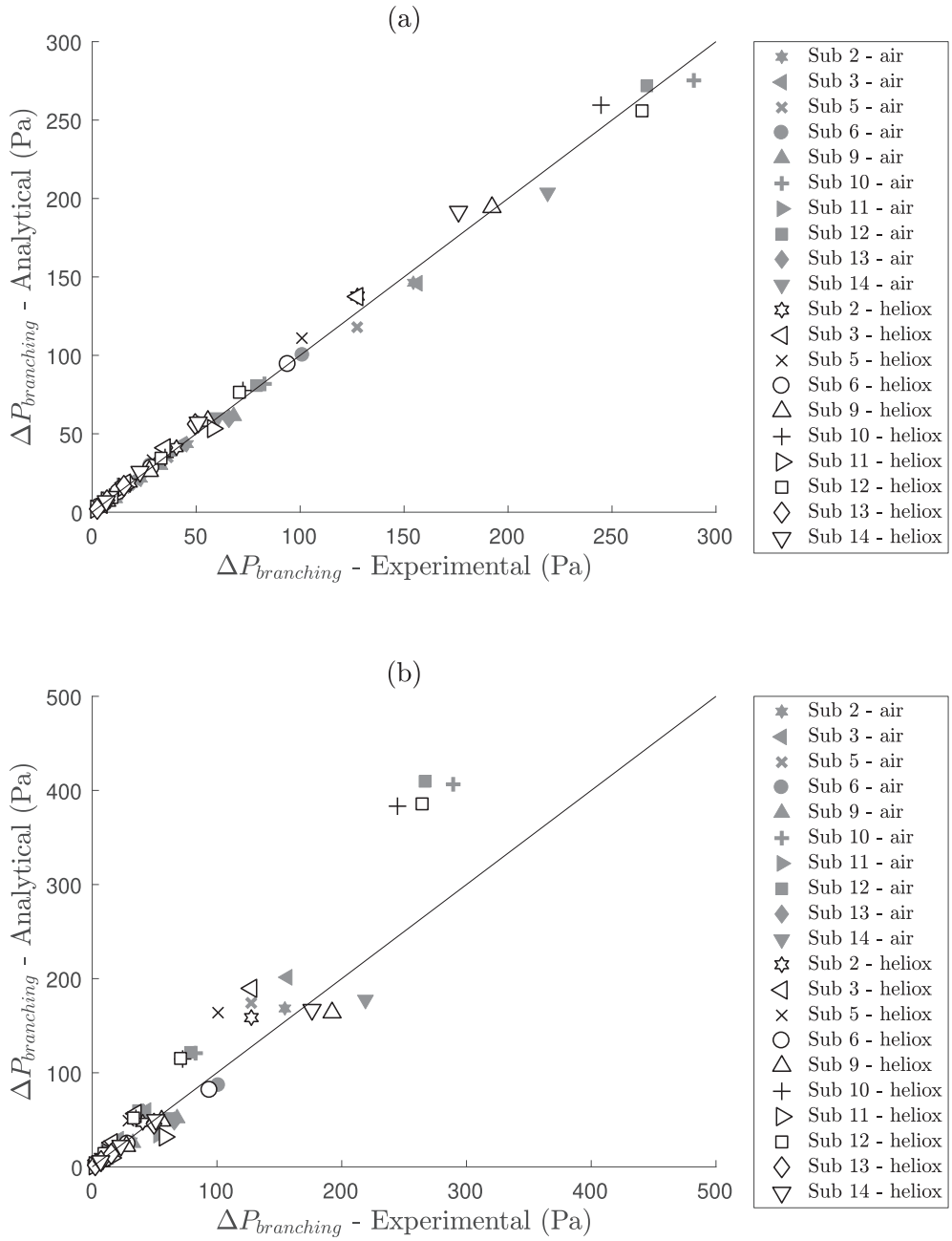

Fig. 4. Branching airways pressure drop using the blasius equation vs. experimental pressure drop; (a) using an ideal C coefficient value for each subject measurements ($\rho_c = 0.997$) and (b) using an average ideal C coefficient value ($\rho_c = 0.909$).

4.1.1. Nose-throat

The average of all fitted α values in Eq. (6) for the nose-throat airways was 0.218. By comparing Eq. (6) with the Blasius equation for pipe friction at low turbulent *Re*, it may be shown that turbulent flow is characterized by $\alpha = 0.25$. The reasonably close agreement between these values is indicative of turbulent flow within the nose-throat airways. Past work in adult nasal airway replicas by Garcia et al. (2009) described pressure drop with an expression analogous to Eq. (6): $\Delta P = aQ^b$, where a and b are constants. From Eqs. (4) and (5), it can be shown that $b = 2 - \alpha$; thus, a value of $\alpha = 0.25$ corresponds to $b = 1.75$. Garcia et al. (2009) determined a range of b values of 1.76–1.85 for four adult replicas at 30–75 L/min flow rates. The range of experimentally determined b values in the present work was 1.70–1.88 (derived from Table 5), showing a notably similar range to that seen by Garcia et al. (2009) and suggesting similar *Re*-dependent flow behavior in their adult and our child nasal airway replicas.

4.1.2. Branching airways

The relationship between C_F and *Re* in the branching airways was investigated in the same manner, where the average α value was found to be 0.238. This α value suggests that turbulence is present in flow through the central branching airways. Much previous work done to model branching airway pressure drop has used the Pedley et al. (1970) equation, for which $\alpha = 0.5$, under the assumption of disturbed laminar flow through branching airways. However, computational fluid dynamics (CFD) studies have indicated that turbulence generated in the upper airways is convected downstream through the central branching airways. For example, a direct numerical simulation (DNS) conducted by Lin et al. (2007) using a realistic adult geometry showed that for a tracheal flow rate of 19.2 L/min ($Re = 1700$) turbulence produced downstream of the glottis constriction influenced flow patterns in the intrathoracic airways. Similarly, simulations in adult airway geometries performed by Xi et al. (2008), Calmet et al. (2016), and Koullapis et al. (2017) demonstrated that turbulence generated in the upper airways influences flow downstream in the branching airways. The results of the present work in airway replicas of children (aged 4–8 years) appear to be consistent with these simulations, in that the relationship between C_F and *Re* indicates the presence of turbulence in the branching airways. Given the tracheal Reynolds number range studied (671–5988 for air and 259–2547 for heliox; Table 4), and increase in total airway cross-section (and hence decrease in *Re*) with each bifurcation, we attribute turbulence in the branching airways mainly to convection of turbulence produced upstream in the upper airway, as opposed to turbulence production in the branching airways, which is also supported by an analysis of turbulent production versus dissipation (Finlay, 2001).

4.1.3. Comparisons of pressure drop for heliox vs. air

Obtaining pressure drop measurements with both air and heliox provided means for an additional method for evaluating flow regime, and defining a model accordingly. Litwin et al. (2017) found the ratio of expected pressure drop at a given flow rate between two fluids is dependent on ρ, μ, and α only. The ratio between pressure drop predicted using the modified-Blasius model in Eq. (13), where $\alpha = 0.25$, for heliox versus air is:

$$\frac{\Delta P_{heliox}}{\Delta P_{air}} = \frac{\left(CRe^{-0.25}\frac{L}{d}\frac{\rho v^2}{2}\right)_{heliox}}{\left(CRe^{-0.25}\frac{L}{d}\frac{\rho v^2}{2}\right)_{air}} = \frac{(\rho^{0.75}\mu^{0.25})_{heliox}}{(\rho^{0.75}\mu^{0.25})_{air}} \quad (14)$$

Thus, based on gas fluid properties described in the methods, the expected pressure drop ratio between heliox and air ($\Delta P_{heliox}/\Delta P_{air}$) is 0.455. The average pressure drop ratio was calculated for each subject, for both branching and nose-throat airways. The overall mean ratios of all subjects and the corresponding standard deviations (representing variation between subjects) are 0.43 ± 0.03 and 0.39 ± 0.03 for branching and nose-throat airways, respectively. The average for each subject was calculated from the pressure drop ratios of the fitted ΔP vs. Q curves for 5–45 L/min (for example, see Fig. 5). Agreement with the ratio of 0.455 predicted analytically is particularly close for the branching airways. In contrast, the ratio predicted by the Pedley et al. (1970) model is 0.625. This provides evidence that the dependence of branching airway pressure drop on gas properties is better predicted using a modified-Blasius turbulent model than using the Pedley et al. (1970) model for the replicas studied here.

4.2. Analytical pressure drop prediction – Absolute values

With the suitability of the modified-Blasius formulation established, an additional aim of the present work was to explore its use in predicting absolute pressure drop values in individual child airways. To fully define the modified-Blasius formulation in Eq. (13), a value for constant C was needed. Initially, subject-specific values, C_{ideal}, were obtained by fitting the experimental data; that is, by optimizing ρ_c as described in the methods. Analytical pressure drop values calculated using C_{ideal} for each subject are com-

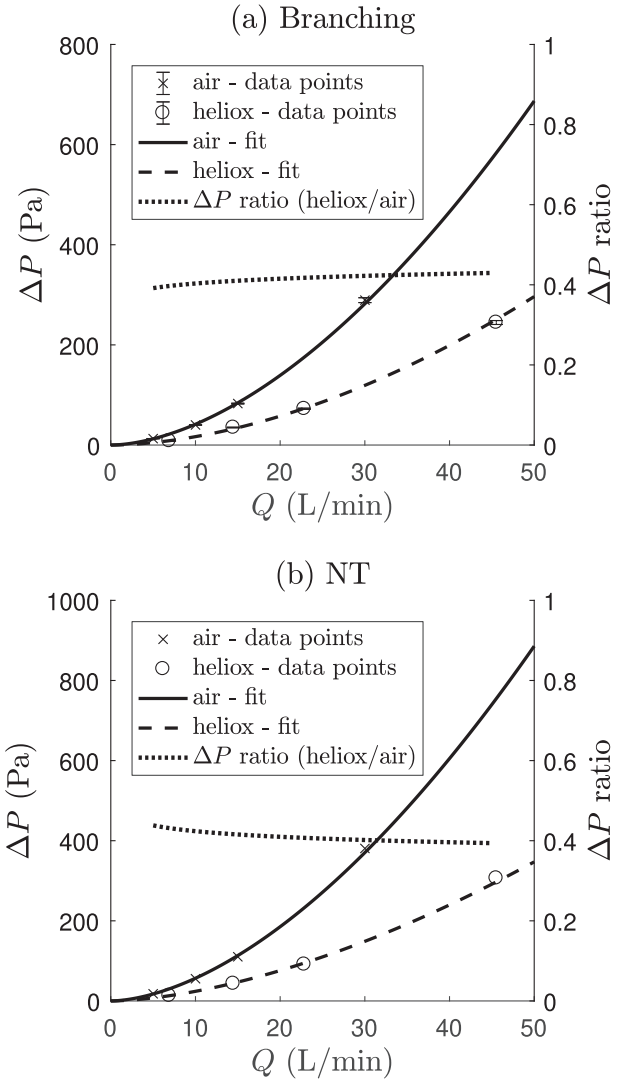

Fig. 5. Pressure drop vs. flow rate for subject 10 in the (a) branching and (b) nose-throat airways with the pressure drop ratio for 5–45 L/min overlaid.

pared with the experimental data in Fig. 4a. The strong correlation ($\rho_c = 0.997$) demonstrates that pressure drop can be accurately predicted using a modified-Blasius formulation, with a single, but subject-specific, coefficient used in each airway segment, and with a constant α value of 0.25. However, it must be emphasized that in the present analysis C_{ideal} was a fit parameter, and no clear correlation between C_{ideal} and subject age, height, weight, trachea length or diameter could be established. It is likely that different values of C_{ideal} for different subjects arise from intersubject variability in more complex features of airway geometry (e.g. branching angles, parent-to-child diameter ratios, asymmetric bifurcations) that are not captured with the parameters listed above.

As an alternative approximation, an average of all C_{ideal} values was calculated as $C_{avg} = 2.98$. Analytical predictions of pressure drop made for all replicas with this single value were considerably less accurate, showing a correlation of $\rho_c = 0.909$ (Fig. 4). Estimation of absolute values of pressure drop through central conducting airways of individual subjects made using the modified-Blasius equation with $C_{avg} = 2.98$ should therefore be done with caution. However, calculation of absolute values of pressure drop for archetypal subjects within the age range studied (4- to 8-years old) may be done so long as airway lengths and diameters are defined.

5. Conclusions

Pressure drop through the nose-throat and central branching airways was measured in airway replicas based on computed tomography (CT) scans of 10 child subjects, between 4- and 8-years old. The relationship between the coefficient of friction, C_F (Slutsky et al., 1980), and Reynolds number, *Re*, was indicative of turbulent flow for both the nose-throat and for the branching airways. The ratio of pressure drop through the branching airways between heliox and air flow was also consistent with predictions made for turbulent flow. The presence of turbulence in the branching airways likely resulted from convection of turbulence produced upstream in the upper airway. An airway resistance model based on the Blasius pipe friction correlation for turbulent flow was proposed for prediction of pressure drop through the bifurcating bronchial airways downstream from the upper airway.

Conflict of interest statement

The authors have no conflict of interest to disclose.

Acknowledgements

AM and WF acknowledge funding from the Canadian Natural Sciences and Engineering Research Council (NSERC). We express our thanks to Fraser Bulbuc, for his enhancements of the 3-D subject geometries and fabrication of replicas.

Appendix A. Supplementary material

Supplementary data to this article can be found online at https://doi.org/10.1016/j.jbiomech.2018.10.028.

References

Bates, A.J., Doorly, D.J., Cetto, R., Calmet, H., Gambaruto, A.M., Tolley, N.S., Houzeaux, G., Schroter, R.C., 2015. Dynamics of airflow in a short inhalation. J. R. Soc. Interface 12.
Blasius, H., 1911. The similarity law in friction processes. Physikalische Zeitschrift 12, 1175–1177.
Borojeni, A.A., Noga, M.L., Martin, A.R., Finlay, W.H., 2015. Validation of airway resistance models for predicting pressure loss through anatomically realistic conducting airway replicas of adults and children. J. Biomech. 48, 1988–1996.
Borojeni, A.A.T., Noga, M.L., Vehring, R., Finlay, W.H., 2014. Measurements of total aerosol deposition in intrathoracic conducting airway replicas of children. J. Aerosol Sci. 73, 39–47.
Calmet, H., Gambaruto, A.M., Bates, A.J., Vázquez, M., Houzeaux, G., Doorly, D.J., 2016. Large-scale CFD simulations of the transitional and turbulent regime for the large human airways during rapid inhalation. Comput. Biol. Med. 69, 166–180.
Damanhuri, N.S., Docherty, P.D., Chiew, Y.S., van Drunen, E.J., Desaive, T., Chase, J.G., 2014. A patient-specific airway branching model for mechanically ventilated patients. Comput. Math. Methods Med. 2014.
Finlay, W.H., 2001. The Mechanics of Inhaled Pharmaceutical Aerosols.
Garcia, G.J.M., Tewksbury, E.W., Wong, B.A., Kimbell, J.S., 2009. Interindividual variability in nasal filtration as a function of nasal cavity geometry. J. Aerosol Med. Pulmonary Drug Deliv. 22, 139–156.
Gemci, T., Ponyavin, V., Chen, Y., Chen, H., Collins, R., 2008. Computational model of airflow in upper 17 generations of human respiratory tract. J. Biomech. 41, 2047–2054.
Katz, I., Caillibotte, G., Martin, A.R., Arpentinier, P., 2011a. Property value estimation for inhaled therapeutic binary gas mixtures: He, Xe, N(2)O, and N(2)with O(2). Med. Gas Res. 1. 28–28.
Katz, I.M., Martin, A.R., Feng, C.-H., Majoral, C., Caillibotte, G., Marx, T., Bazin, J.-E., Daviet, C., 2012. Airway pressure distribution during xenon anesthesia: the insufflation phase at constant flow (volume controlled mode). Appl. Cardiopulm. Pathophysiol. 16.
Katz, I.M., Martin, A.R., Muller, P.A., Terzibachi, K., Feng, C.H., Caillibotte, G., Sandeau, J., Texereau, J., 2011b. The ventilation distribution of helium-oxygen mixtures and the role of inertial losses in the presence of heterogeneous airway obstructions. J. Biomech. 44, 1137–1143.
Koullapis, P.G., Nicolaou, L., Kassinos, S.C., 2017. In silico assessment of mouth-throat effects on regional deposition in the upper tracheobronchial airways. J. Aerosol Sci.
Lawrence, I., Lin, K., 1989. A concordance correlation coefficient to evaluate reproducibility. Biometrics, 255–268.
Lin, C.-L., Tawhai, M.H., McLennan, G., Hoffman, E.A., 2007. Characteristics of the turbulent laryngeal jet and its effect on airflow in the human intra-thoracic airways. Respir. Physiol. Neurobiol. 157, 295–309.
Litwin, P.D., Reis Dib, A.L., Chen, J., Noga, M., Finlay, W.H., Martin, A.R., 2017. Theoretical and experimental evaluation of the effects of an argon gas mixture on the pressure drop through adult tracheobronchial airway replicas. J. Biomech. 58, 217–221.
Pedley, T.J., Schroter, R.C., Sudlow, M.F., 1970. Energy losses and pressure drop in models of human airways. Respir. Physiol. 9, 371–386.
Pozin, N., Montesantos, S., Katz, I., Pichelin, M., Grandmont, C., Vignon-Clementel, I., 2017. Calculated ventilation and effort distribution as a measure of respiratory disease and Heliox effectiveness. J Biomech 60, 100–109.
Slutsky, A.S., Berdine, G.G., Drazen, J.M., 1980. Steady flow in a model of human central airways. J. Appl. Physiol. Respir. Environ. Exerc. Physiol. 49, 417–423.
Storey-Bishoff, J., Noga, M., Finlay, W.H., 2008. Deposition of micrometer-sized aerosol particles in infant nasal airway replicas. J. Aerosol Sci. 39, 1055–1065.
Swan, A.J., Clark, A.R., Tawhai, M.H., 2012. A computational model of the topographic distribution of ventilation in healthy human lungs. J. Theor. Biol. 300, 222–231.
Tgavalekos, N.T., Musch, G., Harris, R., Melo, M.V., Winkler, T., Schroeder, T., Callahan, R., Lutchen, K., Venegas, J., 2007. Relationship between airway narrowing, patchy ventilation and lung mechanics in asthmatics. Eur. Respir. J. 29, 1174–1181.
van Ertbruggen, C., Hirsch, C., Paiva, M., 2005. Anatomically based three-dimensional model of airways to simulate flow and particle transport using computational fluid dynamics. J. Appl. Physiol. 98, 970–980.
White, F.M., 2016. Fluid Mechanics. McGraw-Hill, New York.
Wongviriyawong, C., Harris, R.S., Greenblatt, E., Winkler, T., Venegas, J.G., 2012. Peripheral resistance: a link between global airflow obstruction and regional ventilation distribution. J. Appl. Physiol. 114, 504–514.
Xi, J., Longest, P.W., Martonen, T.B., 2008. Effects of the laryngeal jet on nano-and microparticle transport and deposition in an approximate model of the upper tracheobronchial airways. J. Appl. Physiol. 104, 1761–1777.
Xi, J., Si, X., Kim, J.W., Berlinski, A., 2011. Simulation of airflow and aerosol deposition in the nasal cavity of a 5-year-old child. J. Aerosol Sci. 42, 156–173.